Remote Sensing of Environment 259 (2021) 112418

Contents lists available at ScienceDirect

Remote Sensing of Environment

journal homepage: www.elsevier.com/locate/rse

Blinded evaluation of airborne methane source detection using Bridger Photonics LiDAR

Matthew R. Johnson *, David R. Tyner, Alexander J. Szekeres

Energy & Emissions Research Laboratory, Department of Mechanical and Aerospace Engineering, Carleton University, Ottawa, ON K1S 5B6, Canada

ARTICLE INFO

Editor: Dr. Menghua Wang

Keywords:
Methane
Oil and gas
Mitigation
Regulatory policy
Venting
Fugitive emissions
Inventory
LDAR

ABSTRACT

Controlled, fully-blinded methane releases and ancillary on-site wind measurements were performed during a separate airborne survey of active oil and gas facilities to quantitatively evaluate the capabilities and potential utility of the Bridger Photonics LiDAR-based airborne Gas Mapping LiDAR™ (GML) methane measurement technology under realistic field conditions. Importantly, although Bridger Photonics knew there was a ground team working in the area to deploy wind sensors as part of the broader survey of facilities, they had no knowledge whatsoever that controlled releases were taking place and were not informed of this until all data processing was complete. Thus, the presented data allow a true, fully-blinded assessment of the airborne technology's ability to both detect and locate unknown methane sources within active oil and gas facilities, as well as to quantify their release rates. Results were used to derive a lower-sensitivity limit threshold as a function of wind speed, which matches well with the broader field survey results. Comparison of measurement results with and without the benefit of on-site wind data reveal that uncertainty in the GML source quantification is a direct linear function of the uncertainty in the wind speed. Quantification uncertainties (1σ) of ±31–68% can be expected for sources near the sensitivity limit. The derived sensitivity limit function was incorporated into exploratory simulations using the Fugitive Emissions Abatement Simulation Toolkit (FEAST), which suggest that the Bridger GML technology has comparable performance to optical gas imaging (OGI) camera surveys both in terms of fraction of total emissions detected and anticipated net mitigation. The relative performance of the Bridger GML technology would be expected to improve or worsen as the assumed underlying distribution of source magnitudes becomes more or less positively skewed (i.e. more or less dominated by larger sources such as tank vents). Overall, the Bridger GML technology is shown to be capable of detecting, locating, and quantifying individual sources at or below the magnitudes of recent regulated venting limits. The presented detection sensitivity function will be useful for modelling potential alternate leak detection and repair strategies and interpreting future airborne measurement data.

1. Introduction

Methane is a potent greenhouse gas with a global warming potential many times stronger than that of CO_2. Combined with its comparatively short atmospheric lifetime (~9 years, Myhre et al., 2013), methane is thus a vital target for immediate-term reductions as part of overall objectives of holding planetary warming to <1.5–2 °C (IPCC, 2018). The oil and gas sector is broadly understood as a principal source of anthropogenic methane emissions (IEA, 2020), and recent studies using a range of approaches suggest its contribution to the global balance is underestimated (Alvarez et al., 2018; Hmiel et al., 2020).

Both the United States and Canada have developed methane regulations (ECCC, 2018a; US EPA, 2016) as part of meeting stated policy objectives of reducing oil and gas sector methane emissions by 40–45% by 2025 (Trudeau et al., 2016). Specific regulatory measures vary among provinces and states, (e.g., AER, 2020; BCOGC, 2020; DPHE, 2020; Johnson and Tyner, 2020) but generally include requirements to limit direct venting of methane as well as conduct periodic inspections for fugitive emissions sources (i.e., unintentional venting sources and leaks). Monitoring compliance and tracking the overall impact of regulations toward policy objectives pose a number of technical challenges. Ultimately, these may require one or more of a suite of measurement technologies that together can achieve large-scale aggregate regional emissions measurements, quantification of

* Corresponding author.
E-mail address: Matthew.Johnson@carleton.ca (M.R. Johnson).

https://doi.org/10.1016/j.rse.2021.112418
Received 23 December 2020; Received in revised form 8 March 2021; Accepted 23 March 2021
Available online 31 March 2021

individual site emissions, measurement of emissions from major equipment (e.g. storage tanks, compressor builds, dehydrators, etc.), and measurement of individual emitting components (e.g. pneumatics, valves, fittings, etc.). Several technologies are emerging to meet these needs (Fox et al., 2019; Ravikumar et al., 2019) and recent successful deployments include airborne measurements to quantify "basin-level" emissions from aggregated facilities (e.g. Johnson et al., 2017; Karion et al., 2015; Peischl et al., 2016; Smith et al., 2017), airborne measurement of "facility" or "site-level" emissions (e.g. France et al., 2021; Golston et al., 2018; Gorchov Negron et al., 2020; Mehrotra et al., 2017; Yang et al., 2018), and truck-mounted technologies to screen for emitting sites and/or estimate total site emissions (e.g. Albertson et al., 2016; Atherton et al., 2017; Baillie et al., 2019; Caulton et al., 2019; O'Connell et al., 2019; Rella et al., 2015; Roscioli et al., 2018; Zavala-Araiza et al., 2018). However, for screening potential sources within a facility, optical gas imaging (OGI) via hand-held infrared cameras to reveal otherwise invisible hydrocarbon plumes remains the default approach.

Regulations in several jurisdictions now mandate the use of OGI cameras as part of leak detection and repair (LDAR) programs that are performed at prescribed frequencies ranging from 1 to 12 times per year (AER, 2020; BCOGC, 2020; DPHE, 2020; US EPA, 2016). Recent field research testing the effectiveness of OGI-based LDAR programs, in repeated surveys at the same set of facilities, has affirmed the need for "frequent, effective, and low-cost LDAR surveys" to identify leaks and account for new leaks that occurred between surveys (Ravikumar et al., 2020). However, the overall cost of frequent OGI-LDAR can become quite significant when large numbers of facilities are involved (e.g. ECCC, 2018b). Ravikumar et al. (2020) also found that overall emissions were dominated by intentional or designed releases from sources classed as "vents", especially liquid storage tank vents, rather than those typically classed as fugitive leaks, suggesting a parallel "need for targeted inspections of tanks".

One promising approach for improving efficiency and reducing costs of OGI-LDAR surveys is through the combination of rapid screening approaches with follow-up close-range methods (e.g. Fox et al., 2019; Kemp et al., 2016). Airborne measurement technologies, with the ability to rapidly cover many sites per day, may be especially well-suited to this approach (Schwietzke et al., 2019). Among these, airborne light detection and ranging (LiDAR) technology, which has the potential to detect and quantify major sources within a facility, could be especially advantageous. Recent simulations have shown that airborne LiDAR technology applied with optimized routing could lower inspection costs by up to a factor of six while achieving comparable effectiveness (Rashid et al., 2020). A key aspect of this however is the sensitivity of the measurement system. Simulations using the Fugitive Emissions Abatement Simulation Toolkit (FEAST) suggest that a detection limit between 0.1 and 1 kg/h is sufficient to capture all significant leaks (Ravikumar et al., 2018), where sources below this limit have negligible impact on total emissions. Because surveys are periodic and leaks are dynamic with positively skewed distributions, the fraction of detected emissions "saturates" at a sensitivity of approximately 0.1 kg/h. Thus, depending on the sensitivity of the LiDAR, it may be possible to minimize the need for LDAR inspections, while potentially also targeting the more significant contributions of venting sources noted in recent field work (Ravikumar et al., 2020). The ability to quantify detected sources could also have advantages in assessing compliance with various regulated venting limits (e.g. AER, 2020; ECCC, 2018a) or in jurisdictions where quantification of detected fugitive sources is required (e.g. BCOGC, 2020).

The objective of this paper was to evaluate the performance of new airborne LiDAR technology developed by Bridger Photonics Inc., and in particular, to complete fully-blinded field tests to investigate real-world sensitivity and detection limits. The presented experiments were conducted under cover of a parallel airborne survey of active oil and gas facilities in Northern British Columbia, Canada. As an acknowledged component of this survey, a ground team moved beneath the plane deploying and redeploying wind sensors at a subset of sites with a stated objective of collecting supplementary wind data to assist with the analysis of survey results. However, unbeknownst to Bridger Photonics, the ground crew was also able to perform controlled methane releases at several sites, providing a true, blinded assessment of the sensitivity of the Bridger technology under real-world, oil and gas sector survey conditions. Critically, this enabled a quantitative and fully transparent evaluation of the technology's ability to find sources without knowing where to look or even that an evaluation was underway. These data give unique insight into the current real-world performance of the Bridger system and provide invaluable objective data for understanding the potential utility of this or similar airborne measurement technology. Considering ongoing regulatory development seeking to employ these types of approaches (e.g. AER, 2021), the presented results provide much needed scientifically rigorous data to assist in policy decisions about alternative technologies for finding methane sources, in meeting regulatory requirements, and most importantly, in interpreting field measurement data to develop better inventories and drive mitigation.

2. Methodology

Under the direction of the British Columbia Oil and Gas Research and Innovation Society (BC OGRIS), Bridger Photonics was contracted to complete an aerial survey of 167 oil and gas sites in Northern British Columbia, Canada in September 2019. A research team from the Energy & Emissions Research Lab (EERL) at Carleton University was invited to work in parallel with the aircraft, with goals that included understanding and quantitatively evaluating the capabilities of the airborne measurement system.

2.1. Bridger Photonics airborne measurement technology

Bridger Photonics Inc. Gas Mapping LiDAR™ (GML) technology is an airplane mounted scanning sensor that combines spatially-scanned range-finding and gas-absorbing lasers, a colour frame camera, and a Global Navigation Satellite System - Inertial Navigation System (GNSS-INS) to detect and produce geo-located imagery of methane plumes (Hunter and Thorpe, 2017). Wavelength modulation spectroscopy (WMS) measurements, similar to the technique described in (Iseki et al., 2000), are performed on the methane absorption line at 1651 nm to determine the path-integrated methane concentration between the aircraft and the ground-based topographic backscatterer. The path-integrated methane concentration measurements, derived from the WMS signals, depend on the local atmospheric pressure and temperature, which are measured onboard the GML sensor, the laser modulation parameters, which are calibrated by Bridger Photonics Inc. and verified prior to each flight, and the methane absorption line spectroscopic properties, which are derived from the HITRAN spectroscopic database (Gordon et al., 2017). A model of the WMS LiDAR measurement, similar to the model described in (Iseki et al., 2000), is used to determine the ground reflectivity and the concentration measurement SNR for each measurement. Under nominal operating conditions the path-integrated methane concentration measurements have less than 10% 1σ uncertainty. The range measurement uses frequency-modulated-continuous-wave (FMCW) topographic LiDAR to measure the distance between the aircraft and the ground along the direction of the methane concentration LiDAR measurement (Bridger Photonics, 2021). The topographic LiDAR measurements are combined with the GNSS-INS data to geo-register the topographic and methane concentration LiDAR measurements to a common global coordinate system.

The lasers are rapidly swept in a conical patter which creates an overlapping ellipsoidal pattern on the ground as the airplane flies. For this survey, the GML sensor was deployed on a Cessna 172 and flown with a nominal flight speed of 160 km/h. The sensor field of view was 31° and the nominal flight altitude was 230 m above ground level (AGL); in this configuration, the system measures an approximately 128-m wide LiDAR swath on the ground in a single pass of the airplane. The position

of forward- and backward-looking gas measurements acquired during the flyover are used to determine the plume height, typically to within 2 m. The height-corrected, path-integrated methane concentrations within the laser swath are combined to produce 2D imagery of detected plumes. The spatial resolution of the plume is a function of flight altitude and speed of the aircraft (Hunter and Thorpe, 2017) and was 2 m in the present work. Bridger uses 3D information of the gas plume along with wind speed and other topographic information on the ground to compute the source methane emission rate with an associated 1σ uncertainty of ±30% under typical measurement conditions. The wind speed estimate (See Section 2.2.1) is typically the dominant source of uncertainty in GML emission rate estimates.

Actual in-field site measurement coverage may be impacted by groundcover conditions, e.g. wet soil or standing water which attenuates the LiDAR return signal, or flight path characteristics (e.g. heading, aircraft roll, banking, etc.) during the measurement. Geo-located flight paths and LiDAR return signal coverage, the true laser swath, were provided by Bridger Photonics Inc. allowing an assessment of each site's true measurement area. This was particularly important for analyzing missed controlled releases (see Fig. 2). For locations with detected methane emissions, Bridger Photonics Inc. supplied: i) high resolution site imagery obtained during the survey from an aircraft mounted camera, ii) geo-located methane plume detection imagery from each individual measurement pass, and iii) where possible a plume source location(s) and emission rate(s) in liters per minute (lpm) of methane (at 15°C and 101,325 Pa). In two cases where a controlled release source was measured in two successive and partially overlapping passes of the airplane, the average was used.

2.2. Ground measurements

A ground team of EERL personnel working in 5 trucks was deployed to Northern BC to work concurrently with the airplane. The team's stated goals were to deploy and re-deploy eleven tripod-mounted wind anemometers at as many of the measurement sites in the airborne survey as possible while the plane worked overhead. These data were used to understand the influence of uncertain wind data on the airborne measurement results. However, each truck was also equipped with equipment to perform controlled methane releases enabling independent and objective evaluation of the lower detection limits and measurement uncertainty of Bridger's LiDAR technology. All controlled releases were performed in a true blinded fashion such that Bridger Photonics Inc. had no knowledge that controlled releases were occurring during their separately organized survey of oil and gas facilities in the region, and they were not informed of this until after all data processing was complete. Overall the EERL team was able to catch up with the plane at 48 unique sites completing 65 wind measurements (some sites were visited again by the aircraft on subsequent days) as well as 29 controlled methane releases at 22 distinct sites during the 5-day aerial survey.

2.2.1. Wind data and sensors

Wind data at the source plume height are a necessary component of any source emission rate quantification system and a limit of any remote measurement system. Even at low aircraft altitude, atmospheric effects are such that aircraft measured wind speed and direction can be notably different than those at the plume height (which in the near field, where measurements occur, is generally much closer to the source level on the ground). Typically, when on-site wind measurements are not available, Bridger Photonics Inc. uses interpolated hourly meteorological station data provided by Meteoblue (https://www.meteoblue.com/) to derive local wind information and calculate emission rates from measured methane plume concentrations (ppm·m). The wind speed, u, provided at a reference height of z_1=10 m, is scaled to the measured plume height z_2 via Eq. (1) assuming a standard logarithmic wind profile with a specified zero-displacement plane, d, of 0.066 m and a ground roughness, z_0, of 0.01 m representative of the graded areas around oil and gas infrastructure.

$$u(z_2) = u(z_1)\frac{ln((z_2 - d)/z_0)}{ln((z_1 - d)/z_0)} \quad (1)$$

To evaluate the uncertainties associated with interpolating local wind speed data from available station data as mapped by Meteoblue, emission rate calculations were completed twice – with and without the benefit of site-specific wind speed and direction measurements acquired by the EERL field team. After initial emission calculations were completed by Bridger using interpolated station data, geo-located wind data (speed, direction, sensor height, and location) averaged on 10 s intervals were compiled by EERL and provided to Bridger Photonics and emission results were re-processed.

On-site wind speed and direction data were measured at 1 Hz using tripod-mounted ultrasonic wind sensors. Specifically, a combination of six Anemoment TriSonica Mini Wind and Weather Sensors and five 2D Onset HOBO S-WCG-M003 ultrasonic anemometers were used in the field. Wind sensors were distributed by a ground team of 8 people in 5 trucks equipped with mobile controlled methane release equipment each morning prior to aerial measurements. Typically, an Anemoment sensor (0.1 m/s resolution, ±0.1 m/s accuracy for wind speeds in the 0–10 m/s range) accompanied each mobile methane release while the extra Anemoment and less sensitive Onset sensors (0.4 m/s resolution, max of ±0.8 m/s or 4% of the reading accuracy) were simultaneously deployed at nearby sites. At each location the anemometer was leveled, geo-located by GPS coordinates, positioned at a target height of z_1=3 m above the ground (actual installed heights varied between 2.2 m and 3.6 m to ensure stability for local ground and wind conditions), and orientated to magnetic north using a handheld compass (data were later corrected using a magnetic correction of 17.5 degrees east). The heading and orientation of the Anemoment sensors were additionally checked against internal compass and tilt readings using a laptop and LabVIEW serial interface. As aerial measurements were completed, wind sensors and mobile releases were re-deployed by each truck team ahead of the plane's location as permitted by the daily flight plan.

2.2.2. Mobile controlled methane releases

Methane controlled releases were performed without the knowledge of Bridger Photonics to enable a fully-blinded assessment of the measurement technology near its nominal theoretical lower detection limit of 10 lpm (Hunter and Thorpe, 2017). Controlled releases were completed using calibrated thermal mass flow controllers (Bronkhorst), which we calibrated with bottled methane prior to deployment using a DryCal primary flow calibrator (Mesa labs) with a reference accuracy of 0.15% over a range of 0–50 lpm (0–2 kg/h). In the field, each controlled release was setup alongside an Anemoment wind sensor to log local wind data. Methane release points were geo-located by GPS and installed at a target height between one and two meters above the ground (working height of typical on-site infrastructure). Release flowrates were chosen between 30 and 50 lpm and were continuously monitored by ground personnel allowing visual confirmation of airplane arrival and departure times.

3. Results and discussion

3.1. Influence of wind error on quantified emission rates

The ground team completed 65 separate wind measurements at 48 unique sites, where some sites with detected emissions were revisited on a second day by both the airplane and the ground team. Fig. 1a compares the site-measured wind data with interpolated data derived from Meteoblue. All data are corrected to a common standard height of 3 m. While there is considerable scatter in the data, the on-site results are symmetrically distributed about the 1:1 correspondence line as should be expected. One reason for the large amount of scatter is the difference in the underlying time resolution of the two wind data sets. Meteoblue

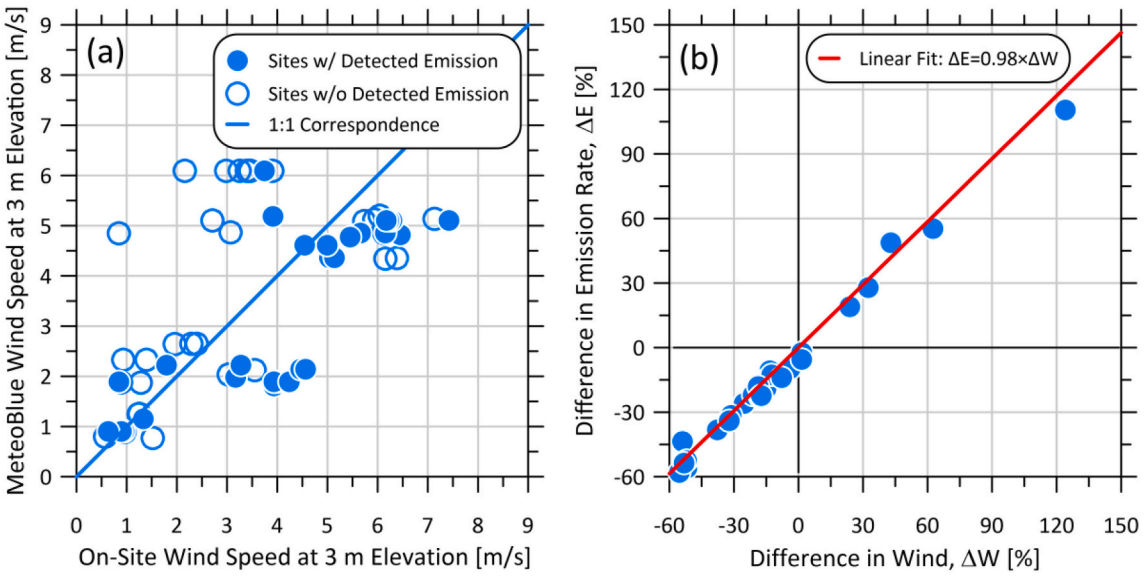

Fig. 1. (a) Comparison of interpolated hourly-averaged Meteoblue wind data with on-site wind anemometer measurements (b) Correspondence between differences in input wind data and calculated emission rates as reported by Bridger indicating a linear dependence of measured emission rate on input wind speed.

data are available as hourly-averaged wind values, which in the present case, Bridger interpolates to derive an average wind speed over a 6-min interval at the time of the aircraft measurement (from 3 min before to 3 min after the flyover time). The EERL on-site wind measurements were provided to Bridger as much higher resolution 10-s averaged data, which Bridger then processed to produce similar 3 to 6-min averages when computing emission rates (i.e. from 3 min before arrival of the plane to the 3 min after or the time data collection was stopped after the plane passed overhead). Thus, the on-site data with an effective resolution of 3–6 min should be expected to capture a much higher level of

Fig. 2. Examples showing possible outcomes of blinded controlled methane releases as seen by the aerial survey. (a) Controlled release plume is visible (blue) and an emission source (number 45 in this example) is correctly identified and quantified near the release location (star). A second emission plume from infrastructure at the site (number 44) is clearly distinguishable from the controlled release plume (b) Controlled release plume is not detected despite confirmation that the plane passed over the source (white lines) and the plume would have been well within the laser swath (pink shading) (c) Controlled release location at the periphery of the facility was at the edge of the laser swath. (For interpretation of the references to colour in this figure legend, the reader is referred to the web version of this article.)

wind variability than the interpolated hourly-averaged Meteoblue data.

Perhaps the more important observation is how changes in input wind speed influence the derived emission rates. For the subset of oil and gas sites where emissions were detected during the broader survey of facilities in Northern BC (filled symbols), Bridger was asked to reprocess their measurements using the site-measured wind data that were subsequently provided by the authors / EERL. Fig. 1b shows the correlation between changes in input wind speed and changes in the derived emission rate of the detected sources. The correspondence is almost perfectly 1:1 suggesting that overall quantification uncertainty is directly proportional to the uncertainty of the available wind data. The data in Fig. 1b also suggest a slight negative bias (underestimate) in the calculated emission rate when using hourly averaged data, with a higher proportion of points falling in the lower-left quadrant of the plot. The distribution of relative wind error is discussed in further detail in Section S1 of the Supplementary Information (SI). The accuracy of the Bridger technology in quantifying the magnitudes of the controlled releases is separately discussed below.

3.2. Controlled release results

To assess whether a controlled release had a fair potential to be detected and quantified by the airplane, release locations, plume imagery, detected source locations, flight paths, and GML laser swath coverage were overlaid with satellite imagery in an ArcGIS environment and individually inspected. Controlled releases were classified into three categories: (i) detected and quantified (11 releases), (ii) missed (10 releases), and (iii) other (8 releases) as explained below.

Fig. 2a shows an example of a successful detection of a controlled release. As in each of the 11 successful detections, the controlled release point (gold star) was well-aligned with Bridger's geo-located detected plume imagery (blue), and was also closely aligned with a Bridger quantified source (labelled as source location 45 in this image). In addition, the controlled release plume was visually distinct from other on-site sources, where in this specific example there was also a detected emission from the facility, labelled as source location 44.

Controlled releases classified as missed had no corresponding plume or detection data but were confirmed to be within the laser swath (i.e. the area with a measurable return signal as indicated by the pink shading). Missed releases were assigned an aerial measurement of 0 kg/h. For the example shown in Fig. 2b, the controlled release location is clearly within the laser measurement swath associated with the three flight passes indicated by the white lines. For missed releases the ground team logs were further checked to verify visual confirmation of the flight passes during the release.

The eight controlled releases falling into the other category included: i) four that were located on the edge of laser swath and where wind conditions at the time of the flight directed the plume outside of the aerial field of view, ii) three release plumes were obscured by other methane plumes being emitted at the site, and iii) one release missed because of an airborne measurement computer malfunction during the flyover. These eight tests were considered as null results and omitted from further analysis. The latter test could arguably have been considered a miss by Bridger, however the airplane was able to reset the system and fly the same site later on. The ground crew had necessarily moved on by this point, so there was no controlled release present during the re-attempt. Similarly, the four missed plumes at the edge of the laser swath (e.g. Fig. 2c) were a result of the ground team not being permitted to access some sites and having to perform releases at the edge of the survey region; this issue is precluded in typical surveys since measurement swaths from different passes overlap within the facility (if more than one pass is necessary).

Fig. 3 compares the controlled methane release rates [kg/h] via the calibrated thermal mass flow controllers (crosses) with the measured rates reported from the aerial survey (circles) for the twenty-one "fair-test" releases (i.e. excluding the eight null releases as described above). The release indices are ordered by increasing controlled release rate and colored by wind speed (corrected to a standard height of 3 m), which varied from 0.5–6.2 m/s across the tests.

In general, the aerial measurements show a clear sensitivity to wind speed and potentially a slight negative bias. The wind speed categorizations in Fig. 3 suggest a course detection break point of approximately 3 m/s (for this range of controlled release rates, but not for the broader survey data as shown in Fig. 5), above which none of the controlled

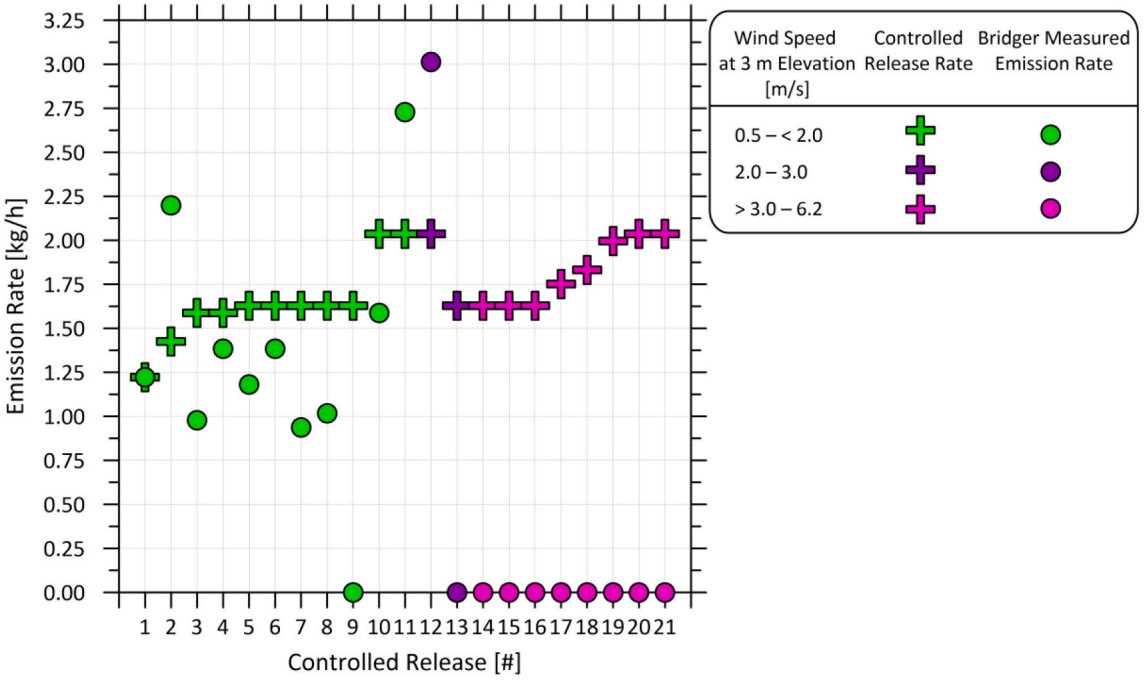

Fig. 3. Comparison of controlled release rates (crosses) with Bridger reported emissions estimates (circles) colored by wind speed. Release indices 11 and 12 are an average of measurements on 2 overlapping airplane passes.

releases were detected. Two 1.6 kg/h releases below 3 m/s were missed, indices 9 and 13, with average wind speeds of 2.0 m/s and 2.7 m/s respectively. A review of ground team logs, wind data, aerial imagery, flight times, and laser return signal imagery confirmed index 9 was a true miss. However, for controlled release index 13, the unaveraged 1 Hz wind data recorded a large gust up to 5.8 m/s with an average of 3.8 m/s in the preceding 10 s before the flyover time, which suggests that the effective wind speed may have been higher than indicated and the plume may not have had time to re-establish during the aerial measurement time.

3.3. Lower sensitivity limits and associated quantification accuracy

An initial estimate of the quantification uncertainty of the Bridger technology near its sensitivity limit was also explored as shown in Fig. 4 and discussed in further detail in the SI. The percent difference between the actual mass flow control release rate and the quantified release emission rate derived using either on-site wind (orange dots) or Meteoblue wind data (blue triangles) is shown on the vertical axis. Note that controlled releases 2 and 8 do not have available ground-team measured wind data—a problem was identified early in the campaign where the memory cards within the data logger could become unseated during transport, which resulted in the loss of on-site wind data for these sites. Releases 1 and 5 had a similar issue but it was possible to determine wind data from a nearby anemometer.

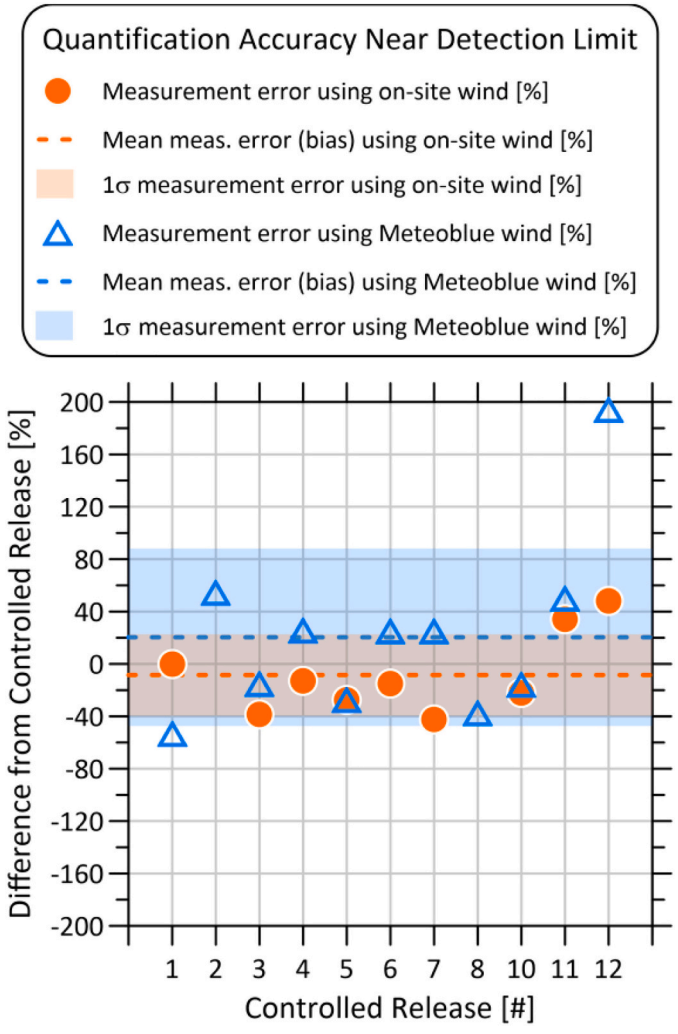

Fig. 4. Error in the Bridger estimates of the controlled release rates (at or near the Bridger sensitivity limit) with and without the benefit of on-site wind measurements.

From the results of Fig. 4, when using the coarser Meteoblue derived wind estimates a 1σ measurement uncertainty of approximately ±68% (blue shading) could be expected for sources at or near the Bridger sensitivity limit. The corresponding dashed line suggests there is also a modest positive bias (overestimation) of +20%. The uncertainties near the sensitivity limit improve when using available on-site wind data, with a 1σ variation of ±31% (orange shading), with a slight negative bias of −8%. These results are discussed in more detail in the SI, which derives probability density functions (Fig. S1) of the expected source quantification error when using either on-site or interpolated Meteoblue wind data to facilitate detailed uncertainty analysis in future measurement surveys. The difference in the two data sets is directly attributable to differences in available wind data uncertainty (bias and precision), which would directly influence the overall measurement uncertainty based on the linear scaling trend of Fig. 1b. The present difference between results with on-site wind and results with interpolated Meteoblue data may also be exacerbated by the challenging terrain in the parts of the measurement region, especially northwest of Fort St. John, BC in the Peace River valley area adjacent to the Rocky Mountains. Moreover, although the sample size of quantified controlled releases is small, these data near Bridger's lower detection limit are useful as a worst case bound for the quantification uncertainty. Measurement uncertainties for larger sources could be expected to be similar or better, up to a point where a plume might be sufficiently optically dense to affect the laser signal.

To further investigate the real-world sensitivity limits of the Bridger technology, the controlled release results of Fig. 3 were recast as a function of windspeed (corrected to a standard height of 3 m) and plotted as blue and red crosses (corresponding to detected or missed releases) in Fig. 5. On their own, these data are sufficient to imply a linear relation between measurement sensitivity (i.e. lower dection limit) and wind speed, especially over the 1.5–3.5 m/s range of wind speeds. However, the broader linear trend becomes much more clear when other data are also considered. The red and blue triangles show further controlled release test data as reported in (Bridger Photonics, 2018) from prior open-field tests. These additional data (conducted at wind speeds between 1 and 2.8 m/s align very well with the present data and implied sensitivity function. From these combined data, a detection sensitivity function was derived using binomial (binary) regression as implemented in Matlab. Several candidate linking functions (i.e. logit, probit, and complementary log-log) were considered and all were statistically justified over a null model (p value <0.05) with nearly identical results. The probit model yielded the minimum deviance and is plotted on Fig. 5. Confidence in this model is further increased when comparing this result with measurements from the parallel survey of active facilities that was the cover for the controlled release experiments.

The grey dots in Fig. 5 correspond to individually quantified methane detections at oil and gas facilities (i.e. non-controlled release sources) within the present northern BC measurement region. (Note: additional detected sources above 7 kg/h are not shown on the plot.) The measured sources similarly align well with the implied sensitivity function, especially at low wind speeds. Although there were three reported sources at higher wind speeds that fell below the suggested sensitivity line; the relative difference for at least two of these points is likely within Bridger's quantification uncertainty. Ideally, further field tests at higher wind speeds could further constrain this new field-derived sensitivity function.

4. Implications

The field-derived detection limit function in kg/h presented in Fig. 5 is the key result for enabling modelling of the effectiveness of a Bridger survey in the context of other or combined approaches to detecting methane sources and/or regulatory limits. For example, newly enacted

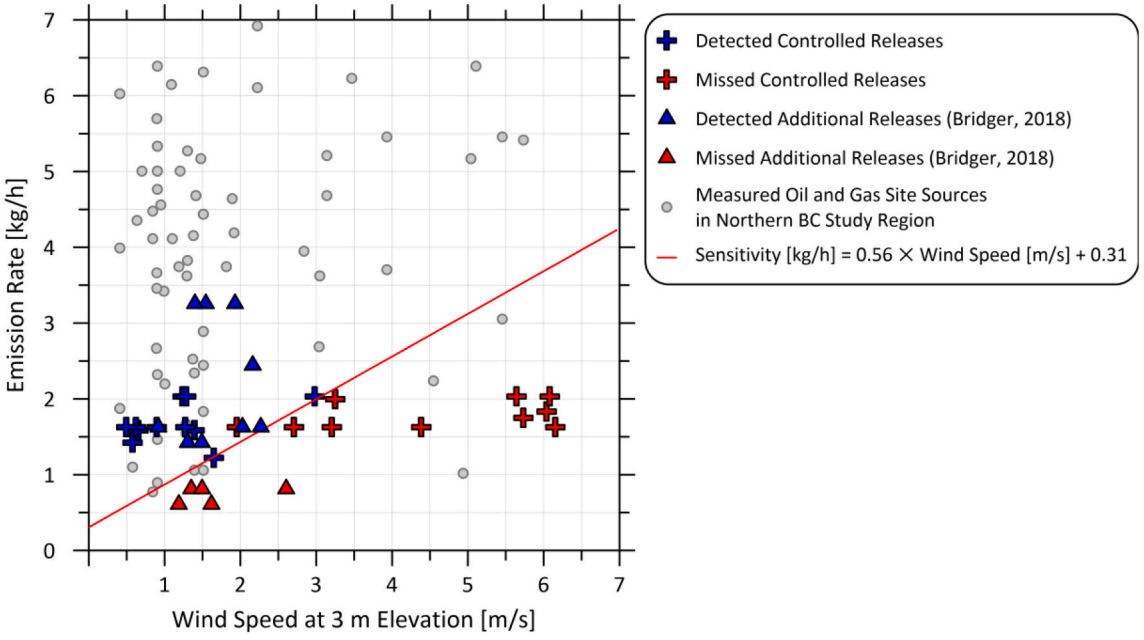

Fig. 5. Field-derived sensitivity limit function of the Bridger GML technology overlaid with the present fully blinded controlled release data, previous release data (Bridger Photonics, 2018), and detected and measured non-controlled released sources from the 167 sites in the northern BC survey.

regulations in Alberta, Canada (AER, 2020) specify and overall site vent gas limit (OVG) of 12.3 kg/h of methane (specified in the regulation as both 9000 kg/mo of methane or 15,000 m^3/mo of gas). For new sites, there is a separate "defined vent gas" (DVG) limit of 2.46 kg/h (written as 1800 kg/mo of methane or 3000 m^3/mo of gas). The derived sensitivity function shown in Fig. 5 suggests the current iteration of the Bridger technology is sufficient to assess both these limits (notwithstanding additional considerations of survey frequency as also disussed below). Similarly, regulations in U.S. states such as Oklahoma, Kanasa, Wyoming, and Utah (Kansas, 2015; Oklahoma Register, 2020; Utah, 2020; WOGCC, 2016) permit venting at the well head of up to 20–60 mcfd (equivalent to ~14–42 kg/h of methane), which again is much higher than the derived sensitivity limit. Alternatively, Canadian federal regulations (ECCC, 2018a) specify a site venting limit of 15,000 m^3/yr (which excludes some sources captured in Alberta's OVG, Johnson and Tyner, 2020). Assuming the same implicit gas composition as in the AER regulations, this is equivalent to approximately 1.03 kg/h, which may be just beyond the capabilites of the current Bridger system except at low ground wind speeds or with possible compromises on flight speed, altitude, and laser swath coverage. It should also be noted however, that through approved or pending equivalency agreements, the ECCC regulations are currently superseded by provincial regulations in Alberta, British Columbia, and Saskatchewan, which in 2019 were collectively reponsible for 98% of all onshore oil and 100% of all gas production in Canada (CER, 2020a, 2020b).

Finally, preliminary simulations were performed using the FEAST

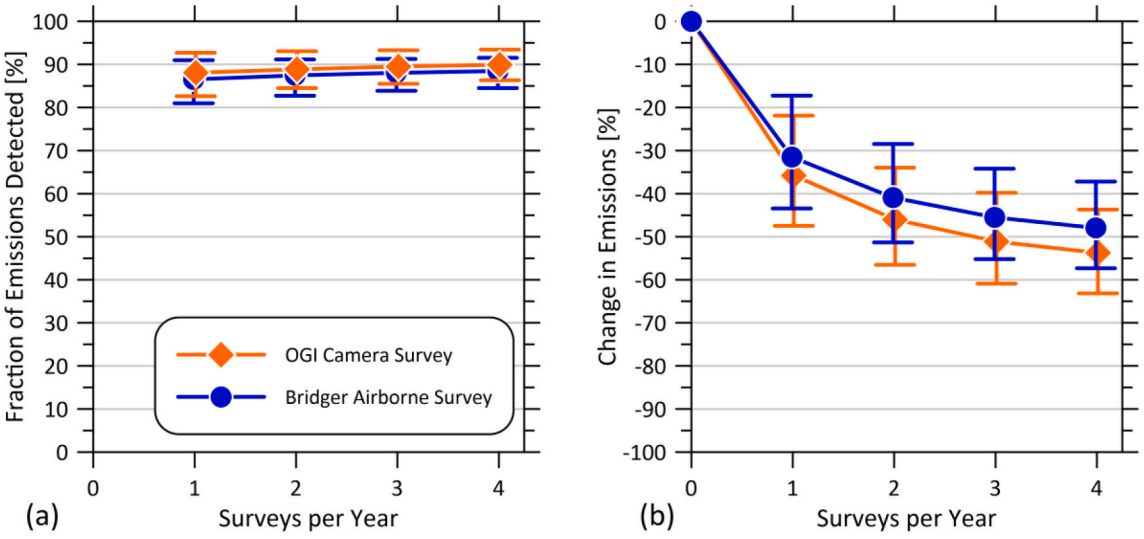

Fig. 6. Reference case FEAST simulation results comparing the performance of standard OGI surveys with the Bridger airborne technology incorporating the derived sensitivity limit function of Fig. 5. The reader is reminded that these reference simulations are based on default values in FEAST 2.0 for a gas field in Texas and results would be expected to vary as the underlying distribution of sources and leak occurrence rates changes. (a) Fraction of total methane emissions that are detected with either approach (b) Modelled expected emissions reductions relative to the Null-repair scenario in FEAST. Vertical error bars indicate the 95% confidence intervals of the simulation results.

2.0 simulation toolkit (Kemp et al., 2016) to model the potential utility of the Bridger technology based on the field-derived sensitivity function of Fig. 5. The simulations were run using the default leak generation and wind data for the Fort Worth, Texas area. The gas field simulated is composed of 100 gas well sites with an average of 650 components per site. No parameters were changed from the default settings with the exception of reducing the duration of each simulation from 10 years to 8 years similar to the procedure followed in Ravikumar and Brandt (2017). A custom leak detection program module was added to simulate the Bridger technology. Default wind data within FEAST are at 2-m height and the same log-profile function (1) was used to convert these to wind speeds at 3-m height (corresponding to the sensitivity function of Fig. 5) within the code. Fig. 6 compares simulated performance of the Bridger technology with standard OGI camera surveys at frequencies of 1–4 times per year.

The proportion of detected emissions using either the OGI or Bridger aproaches (Fig. 6a) are comparable in these simulated scenarios, with substantial overlap of the 95% confidence intervals of the individual realizations within the simulation as indicated by the vertical error bars. However, in this default scenario, a majority of the detected emissions in either case are attributable to normal maintenance and operational practices. As expected, increased survey frequency results in a greater proportion of emissions being detected whether it is for the OGI camera or the Bridger technology survey.

Fig. 6b shows the modelled emissions reductions that could be expected at different survey frequencies. The difference between Fig. 6a and b is due to the reoccurrence or occurence of new leaks in the simulations and highlights the importance of more frequent surveys in reducing emissions (e.g. Ravikumar et al., 2020; Ravikumar and Brandt, 2017). Although OGI achieves up to 6% greater reductions in this reference scenario, there is again significant overlap in the 95% confidence intervals of the two techologies. The relative performance of the Bridger technology is dependent on the assumed simulation parameters and would be expected to improve or worsen if the assumed underlying source distribution was more or less positively skewed. Stated another way, the relative performance of the Bridger technology would be expected to improve in scenarios where emissions are more dominated by larger unmeasured vented sources such as liquid storage tanks. In this context, recent long-duration measurements at 36 natural gas facilities in Alberta, Canada, found that “tanks are the largest single emission source” with a mean emission rate of 52 kg/day and a 90% cut-off at 25 kg CH_4/d (Ravikumar et al., 2020). The majority of these sources would be well above the field-derived sensitivity limit of approximately 1 kg/h derived in the present work. Using a different aerially guided leak detection approach (Schwietzke et al., 2019) observed “that fixable CH_4 emissions per O&G production facility determined from the aerial approach are up to an order of magnitude greater compared with ground-based detects”. Overall, the present results suggest that airborne LiDAR measurements could be a valuable tool in mitigating oil and gas sector methane emissions and the field-derived sensitivity limit function should be valuable in future measurement and modelling efforts.

5. Conclusions

Fully-blinded controlled release tests in conjunction with a parallel airborne survey of active oil and gas facilities were used to evaluate the performance of the Bridger Gas Mapping LiDAR™ technology in both detecting and locating unknown methane emissions sources within active oil and gas facilities as well as quantifying emission rates. Results were used to derive a wind-speed dependent lower sensitivity limit function that will be valuable for interpreting field measurement data as well as modelling of the GML technology as part of alternate leak detection and repair strategies. The field-derived sensitivity limit of approximately 1 kg/h depending on conditions is comparable or lower than venting limits put forward in recent methane regulations. Quantification uncertainty is revealed to be a direct function of the uncertainty in available wind speed data, where 1σ uncertainties of ±31–68% can be expected for sources near the sensitivity limit. Preliminary FEAST simulations incorporating the sensitivity limit function suggest that the Bridger technology could perform comparably with OGI surveys at equivalent frequencies. However, the relative performance should be expected to vary with changes in the underlying model assumptions about source distributions. Most importantly, the presented results and sensitivity function can be used to interpret future field measurement data using this technology and should enable renewed model assessments under a range of scenarios as understanding of oil and gas sector emissions patterns continues to evolve.

Funding

This work was supported by British Columbia Oil and Gas Research and Innovation Society (BCOGRIS, contract number ER-Meth-2020-02a), Natural Resources Canada (grant number EIP2-MET-001), and the Natural Sciences and Engineering Research Council of Canada (NSERC, grant numbers 06632 and 522658).

Declaration of Competing Interest

The authors have no competing interests to declare.

Acknowledgements

This project was undertaken with the support of the BC Oil and Gas Methane Emissions Research Collaborative (MERC) as part of an overall research plan focused on methane emissions from the oil and gas sector in BC and was possible only through the leadership of Don D’Souza (BC Ministry of Environment and Climate Change Strategy) and Marie Johnson (BC Oil & Gas Commission). We are especially grateful to members of the Energy & Emissions Research Lab (EERL) who were able to come together on such short notice to successfully complete the initial field components of the work. The patient assistance of Dr. Mike Thorpe (Bridger Photonics) in processing and re-processing analysis results without and with supplementary ground wind measurements we provided is gratefully acknowledged, as is his professionalism and commitment to the integrity of the project once we were finally able to reveal the blinded release component of the work. The cooperation of the flight team in the field was a key part of our being able to deploy and redeploy wind sensors as the plane moved and ultimately to succeed in deploying the blinded controlled releases. We also gratefully acknowledge the help of Dr. Bradley Conrad in deriving the probability density functions (SI) and running the binomial regression in Matlab. Finally, the forward-thinking support of Michael Layer (Natural Resources Canada) was essential to leveraging resources and expertise for the initial rapid deployment to the field.

Appendix A. Supplementary data

Supplementary data to this article can be found online at https://doi.org/10.1016/j.rse.2021.112418.

References

AER, 2020. Directive 060 (Effective May 2020) [WWW Document]. Calgary, AB. URL. https://www.aer.ca/documents/directives/Directive060_2020.pdf.

AER, 2021. Alternative Fugitive Emission Management Program Approvals [WWW Document]. URL. https://www.aer.ca/protecting-what-matters/holding-industry-accountable/industry-performance/methane-performance/alternative-fugitive-emission-management-program-approvals (accessed 2.15.21).

Albertson, J.D., Harvey, T., Foderaro, G., Zhu, P., Zhou, X., Ferrari, S., Amin, M.S., Modrak, M., Brantley, H.L., Thoma, E.D., 2016. A mobile sensing approach for regional surveillance of fugitive methane emissions in oil and gas production. Environ. Sci. Technol. 50, 2487–2497. https://doi.org/10.1021/acs.est.5b05059.

Alvarez, R.A., Zavala-Araiza, D., Lyon, D.R., Allen, D.T., Barkley, Z.R., Brandt, A.R., Davis, K.J., Herndon, S.C., Jacob, D.J., Karion, A., Kort, E.A., Lamb, B.K., Lauvaux, T., Maasakkers, J.D., Marchese, A.J., Omara, M., Pacala, S.W., Peischl, J.,

Robinson, A.L., Shepson, P.B., Sweeney, C., Townsend-Small, A., Wofsy, S.C., Hamburg, S.P., 2018. Assessment of methane emissions from the U.S. oil and gas supply chain. Science (80-.) 361, 186–188. https://doi.org/10.1126/science.aar7204.

Atherton, E., Risk, D., Fougère, C., Lavoie, M., Marshall, A., Werring, J., Williams, J.P., Minions, C., 2017. Mobile measurement of methane emissions from natural gas developments in northeastern British Columbia, Canada. Atmos. Chem. Phys. 17, 12405–12420. https://doi.org/10.5194/acp-17-12405-2017.

Baillie, J., Risk, D., Atherton, E., O'Connell, E., Fougère, C., Bourlon, E., MacKay, K., 2019. Methane emissions from conventional and unconventional oil and gas production sites in southeastern Saskatchewan, Canada. Environ. Res. Commun. 1, 011003 https://doi.org/10.1088/2515-7620/ab01f2.

BCOGC, 2020. Oil and Gas Activities Act Drilling and Production Regulation. British Columbia Oil and Gas Commission, British Columbia.

Bridger Photonics, 2018. Gas mapping LiDAR for airborne methane leak detection, localiziation and quantification. In: PTAC 2018 Methane Emissions Reduction Forum. Petroleum Technology Alliance of Canada (PTAC), Banff, Alberta.

Bridger Photonics, 2021. Bridger Photonics FMCW LiDAR [WWW Document]. URL. https://www.bridgerphotonics.com/blog/frequency-modulated-continuous-wave-fmcw-lidar (accessed 3.3.21).

Caulton, D.R., Lu, J.M., Lane, H.M., Buchholz, B., Fitts, J.P., Golston, L.M., Guo, X., Li, Q., McSpiritt, J., Pan, D., Wendt, L., Bou-Zeid, E., Zondlo, M.A., 2019. Importance of Superemitter natural gas well pads in the Marcellus shale. Environ. Sci. Technol. 53, 4747–4754. https://doi.org/10.1021/acs.est.8b06965.

CER, 2020a. 2019 Marketable Natural Gas Production in Canada [WWW Document]. URL. https://www.cer-rec.gc.ca/en/data-analysis/energy-commodities/natural-gas/statistics/marketable-natural-gas-production-in-canada.html.

CER, 2020b. 2019 Estimated Production of Canadian Crude Oil and Equivalent [WWW Document]. URL. https://www.cer-rec.gc.ca/en/data-analysis/energy-commodities/crude-oil-petroleum-products/statistics/estimated-production-canadian-crude-oil-equivalent.html.

DPHE, 2020. Regulation no. In: 7, Control of Ozone Via Ozone Precursors and Control of Hydrocarbons Via Oil and Gas Emissions. Department of Public Health And Environment (DPHE), Colorado.

ECCC, 2018a. Regulations Respecting Reduction in the Release of Methane and Certain Volatile Organic Compounds (Upstream Oil and Gas Sector). Environment and Climate Change Canada (ECCC), Canada.

ECCC, 2018b. Regulatory impact analysis statement. Canada Gaz. 152, 1–101.

Fox, T.A., Barchyn, T.E., Risk, D., Ravikumar, A.P., Hugenholtz, C.H., 2019. A review of close-range and screening technologies for mitigating fugitive methane emissions in upstream oil and gas. Environ. Res. Lett. 14, 053002 https://doi.org/10.1088/1748-9326/ab0cc3.

France, J.L., Bateson, P., Dominutti, P., Allen, G., Andrews, S., Bauguitte, S., Coleman, M., Lachlan-Cope, T., Fisher, R.E., Huang, L., Jones, A.E., Lee, J., Lowry, D., Pitt, J., Purvis, R., Pyle, J., Shaw, J., Warwick, N., Weiss, A., Wilde, S., Witherstone, J., Young, S., 2021. Facility level measurement of offshore oil and gas installations from a medium-sized airborne platform: method development for quantification and source identification of methane emissions. Atmos. Meas. Tech. 14, 71–88. https://doi.org/10.5194/amt-14-71-2021.

Golston, L.M., Aubut, N.F., Frish, M.B., Yang, S., Talbot, R.W., Gretencord, C., McSpiritt, J., Zondlo, M.A., 2018. Natural gas fugitive leak detection using an unmanned aerial vehicle: Localization and quantification of emission rate. Atmosphere (Basel) 9. https://doi.org/10.3390/atmos9090333.

Gorchov Negron, A.M., Kort, E.A., Conley, S.A., Smith, M.L., 2020. Airborne assessment of methane emissions from offshore platforms in the U.S. Gulf of Mexico. Environ. Sci. Technol. 54, 5112–5120. https://doi.org/10.1021/acs.est.0c00179.

Gordon, I.E., Rothman, L.S., Hill, C., Kochanov, R.V., Tan, Y., Bernath, P.F., Birk, M., Boudon, V., Campargue, A., Chance, K.V., Drouin, B.J., Flaud, J.-M., Gamache, R.R., Hodges, J.T., Jacquemart, D., Perevalov, V.I., Perrin, A., Shine, K.P., Smith, M.-A.H., Tennyson, J., Toon, G.C., Tran, H., Tyuterev, V.G., Barbe, A., Császár, A.G., Devi, V. M., Furtenbacher, T., Harrison, J.J., Hartmann, J.-M., Jolly, A., Johnson, T.J., Karman, T., Kleiner, I., Kyuberis, A.A., Loos, J., Lyulin, O.M., Massie, S.T., Mikhailenko, S.N., Moazzen-Ahmadi, N., Müller, H.S.P., Naumenko, O.V., Nikitin, A. V., Polyansky, O.L., Rey, M., Rotger, M., Sharpe, S.W., Sung, K., Starikova, E., Tashkun, S.A., Auwera, J. Vander, Wagner, G., Wilzewski, J., Wcisło, P., Yu, S., Zak, E.J., 2017. The HITRAN2016 molecular spectroscopic database. J. Quant. Spectrosc. Radiat. Transf. 203, 3–69. https://doi.org/10.1016/j.jqsrt.2017.06.038.

Hmiel, B., Petrenko, V.V., Dyonisius, M.N., Buizert, C., Smith, A.M., Place, P.F., Harth, C., Beaudette, R., Hua, Q., Yang, B., Vimont, I., Michel, S.E., Severinghaus, J.P., Etheridge, D., Bromley, T., Schmitt, J., Faïn, X., Weiss, R.F., Dlugokencky, E., 2020. Preindustrial 14CH4 indicates greater anthropogenic fossil CH4 emissions. Nature 578, 409–412. https://doi.org/10.1038/s41586-020-1991-8.

Hunter, D., Thorpe, M., 2017. Gas Mapping LiDAR Aerial Verification Program Final Report [WWW Document]. Alberta Upstream Petroleum Research Fund Project 17-ARPC-03, Petroleum Technology Alliance of Canada (PTAC). URL. https://auprf.ptac.org/wp-content/uploads/2018/08/17-ARPC-03-Gas-Mapping-LiDAR-Report-180417v2.pdf.

IEA, 2020. Methane Tracker 2020 [WWW Document]. URL. https://www.iea.org/reports/methane-tracker-2020.

IPCC, 2018. Summary for policymakers. In: Masson-Delmotte, V., Zhai, P., Pörtner, H.-O., Roberts, D., Skea, J., Shukla, P.R., Waterfield, T. (Eds.), Global Warming of 1.5°C. An IPCC Special Report on the Impacts of Global Warming of 1.5°C above Pre-Industrial Levels and Related Global Greenhouse Gas Emission Pathways, in the Context of Strengthening the Global Response to the Threat of Climate Change.

Iseki, T., Hideo, T., Kimura, K., 2000. A portable remote methane sensor using a tunable diode laser. Meas. Sci. Technol. 11, 594–602. https://doi.org/10.1088/0957-0233/11/6/302.

Johnson, M.R., Tyner, D.R., 2020. A case study in competing methane regulations: will Canada's and Alberta's contrasting regulations achieve equivalent reductions? Elem. Sci. Anth. 8, 14. https://doi.org/10.1525/elementa.403.

Johnson, M.R., Tyner, D.R., Conley, S.A., Schwietzke, S., Zavala-Araiza, D., 2017. Comparisons of airborne measurements and inventory estimates of methane emissions in the Alberta upstream oil and gas sector. Environ. Sci. Technol. 51, 13008–13017. https://doi.org/10.1021/acs.est.7b03525.

Kansas, 2015. 82–3-208. Venting or flaring of casinghead gas.

Karion, A., Sweeney, C., Kort, E.A., Shepson, P.B., Brewer, A., Cambaliza, M., Conley, S. A., Davis, K., Deng, A., Hardesty, M., Herndon, S.C., Lauvaux, T., Lavoie, T., Lyon, D. R., Newberger, T., Ptron, G., Rella, C., Smith, M., Wolter, S., Yacovitch, T.I., Tans, P., 2015. Aircraft-based estimate of total methane emissions from the Barnett Shale Region. Environ. Sci. Technol. 49, 8124–8131. https://doi.org/10.1021/acs.est.5b00217.

Kemp, C.E., Ravikumar, A.P., Brandt, A.R., 2016. Comparing natural gas leakage detection technologies using an open-source "virtual gas field" simulator. Environ. Sci. Technol. 50, 4546–4553. https://doi.org/10.1021/acs.est.5b06068.

Mehrotra, S., Faloona, I., Suard, M., Conley, S., Fischer, M.L., 2017. Airborne methane emission measurements for selected oil and gas facilities across California. Environ. Sci. Technol. 51, 12981–12987. https://doi.org/10.1021/acs.est.7b03254.

Myhre, G., Shindell, D.T., Bréon, F.-M., Collins, W., Fuglestvedt, J., Huang, J., Koch, D., Lamarque, J.-F., Lee, D., Mendoza, B., Nakajima, T., Robock, A., Stephens, G., Takemura, T., Zhang, H., IPCC, 2013. Anthropogenic and natural radiative forcing. In: Stocker, T.F., Qin, D., Plattner, G.-K., Tignor, M., Allen, S.K., Boschung, J., Midgley, P.M. (Eds.), Climate Change 2013: The Physical Science Basis. Contribution of Working Group I to the Fifth Assessment Report of the Intergovernmental Panel on Climate Change. Cambridge University Press, Cambridge, United Kingdom and New York, NY, USA, pp. 659–740.

O'Connell, E., Risk, D., Atherton, E., Bourlon, E., Fougère, C., Baillie, J., Lowry, D., Johnson, J., 2019. Methane emissions from contrasting production regions within Alberta, Canada: implications under incoming federal methane regulations. Elem. Sci. Anth. 7, 1–13. https://doi.org/10.1525/elementa.341.

Oklahoma Register, 2020. Title 165: Corporation Commission Chapter 10: Oil and Gas Conservation 165:10–3-15. Venting and flaring.

Peischl, J., Karion, A., Sweeney, C., Kort, E.A., Smith, M.L., Brandt, A.R., Yeskoo, T., Aikin, K.C., Conley, S.A., Gvakharia, A., Trainer, M., Wolter, S., Ryerson, T.B., 2016. Quantifying atmospheric methane emissions from oil and natural gas production in the Bakken shale region of North Dakota. J. Geophys. Res. Atmos. 121, 6101–6111. https://doi.org/10.1002/2015JD024631.

Rashid, K., Speck, A., Osedach, T.P., Perroni, D.V., Pomerantz, A.E., 2020. Optimized inspection of upstream oil and gas methane emissions using airborne LiDAR surveillance. Appl. Energy 275, 115327. https://doi.org/10.1016/j.apenergy.2020.115327.

Ravikumar, A.P., Brandt, A.R., 2017. Designing better methane mitigation policies: the challenge of distributed small sources in the natural gas sector. Environ. Res. Lett. 12 https://doi.org/10.1088/1748-9326/aa6791.

Ravikumar, A.P., Wang, J., McGuire, M., Bell, C.S., Zimmerle, D.J., Brandt, A.R., 2018. "Good versus good enough?" empirical tests of methane leak detection sensitivity of a commercial infrared camera. Environ. Sci. Technol. 52, 2368–2374. https://doi.org/10.1021/acs.est.7b04945.

Ravikumar, A.P., Sreedhara, S., Wang, J., Englander, J.G., Roda-Stuart, D., Bell, C.S., Zimmerle, D.J., Lyon, D., Mogstad, I., Ratner, B., Brandt, A.R., 2019. Single-blind inter-comparison of methane detection technologies – results from the Stanford/EDF mobile monitoring challenge. Elem. Sci. Anth. 7, 37. https://doi.org/10.1525/elementa.373.

Ravikumar, A.P., Roda-Stuart, D., Liu, R., Bradley, A., Bergerson, J., Nie, Y., Zhang, S., Bi, X., Brandt, A.R., 2020. Repeated leak detection and repair surveys reduce methane emissions over scale of years. Environ. Res. Lett. 15 https://doi.org/10.1088/1748-9326/ab6ae1.

Rella, C.W., Tsai, T.R., Botkin, C.G., Crosson, E.R., Steele, D., 2015. Measuring Emissions from oil and Natural gas well pads using the mobile Flux plane technique. Environ. Sci. Technol. 49, 4742–4748. https://doi.org/10.1021/acs.est.5b00099.

Roscioli, J.R., Herndon, S.C., Yacovitch, T.I., Knighton, W.B., Zavala-Araiza, D., Johnson, M.R., Tyner, D.R., 2018. Characterization of methane emissions from five cold heavy oil production with sands (CHOPS) facilities. J. Air Waste Manage. Assoc. 68, 671–684. https://doi.org/10.1080/10962247.2018.1436096.

Schwietzke, S., Harrison, M., Lauderdale, T., Branson, K., Conley, S., George, F.C., Jordan, D., Jersey, G.R., Zhang, C., Mairs, H.L., Pétron, G., Schnell, R.C., 2019. Aerially guided leak detection and repair: a pilot field study for evaluating the potential of methane emission detection and cost-effectiveness. J. Air Waste Manage. Assoc. 69, 71–88. https://doi.org/10.1080/10962247.2018.1515123.

Smith, M.L., Gvakharia, A., Kort, E.A., Sweeney, C., Conley, S.A., Faloona, I.C., Newberger, T., Schnell, R., Schwietzke, S., Wolter, S., 2017. Airborne quantification of methane emissions over the Four Corners region. Environ. Sci. Technol. https://doi.org/10.1021/acs.est.6b06107 acs.est.6b06107.

Trudeau, J., Obama, B., Nieto, E.P., 2016. Leaders' Statement on a North American Climate, Clean Energy, and Environment Partnership [WWW Document]. URL. https://pm.gc.ca/eng/news/2016/06/29/leaders-statement-north-american-climate-clean-energy-and-environment-partnership.

US EPA, 2016. NSPS OOOOa: oil and natural gas sector: emission standards for new, reconstructed, and modified sources; final rule. Fed. Regist. 81, 35824–35942.

Utah, 2020. R649-3: Drilling and Operating Practices.

WOGCC, 2016. Wyoming Oil and Gas Conservation Commission Ch. 3, Sec. 39, Authorization for Flaring and Venting Gas. Wyoming Oil & Gas Conservation Commission (WOGCC).

Yang, S., Talbot, R.W., Frish, M.B., Golston, L.M., Aubut, N.F., Zondlo, M.A., Gretencord, C., McSpiritt, J., 2018. Natural gas fugitive leak detection using an unmanned aerial vehicle: measurement system description and mass balance approach. Atmosphere (Basel) 9. https://doi.org/10.3390/atmos9100383.

Zavala-Araiza, D., Herndon, S.C., Roscioli, J.R., Yacovitch, T.I., Johnson, M.R., Tyner, D. R., Omara, M., Knighton, B., 2018. Methane emissions from oil and gas production sites in Alberta, Canada. Elem. Sci. Anthr. 6, 1–13. https://doi.org/10.1525/elementa.284.